JOURNAL OF MAGNETIC RESONANCE **124,** 400–409 (1997)
ARTICLE NO. MN961043

The Use of Continuous Regularization in the Automated Analysis of MRS Time-Domain Data

JENS TOTZ,* AAD VAN DEN BOOGAART,† SABINE VAN HUFFEL,‡ DANIELLE GRAVERON-DEMILLY,§ IOANNIS DOLOGLOU,¶ RALF HEIDLER,* AND DIETER MICHEL*

**Fakultät für Physik und Geowissenschaften, Universität Leipzig, Linnéstrasse 5, D-04103 Leipzig, Germany; †Biomedical NMR Unit, Department of Radiology, Faculty of Medicine, Katholieke Universiteit Leuven, Gasthuisberg, 3000 Leuven, Belgium; ‡Department of Electrical Engineering (ESAT), Katholieke Universiteit Leuven, Kardinaal Mercierlaan 94, 3001 Leuven-Heverlee, Belgium; §Laboratoire de RMN, CNRS UPRESA 5012, Université Lyon I-CPE, 43 Boulevard du 11 Novembre 1918, 69622 Villeurbanne Cedex, France; and ¶National Technical University of Athens, 9 Iroon Polytechniou Street, Zographou 15773, Greece*

Received March 18, 1996; revised October 18, 1996

In this paper, it is shown how the advantages of continuous regularization (CR) can be exploited to achieve an improved, fully automated LPSVD analysis of MRS time-domain data. The main advantage of CR is its ability to determine the number of spectral components even at low signal-to-noise ratios, which suggested its use for *in vivo* spectroscopy. Estimation of the spectral parameters is possible. Two alternatives of automated data-analysis schemes are thoroughly investigated by means of Monte Carlo studies. The results suggest the combination of CR for model-order estimation with other methods for more-accurate parameter estimation. Several possible combinations, including those with an improved enhancement procedure and a total-least-squares method for quantitation, are discussed. Recommendations are given for spectral analysis, and a new data-analysis protocol which performs significantly better than previously used protocols of the same type is proposed.

INTRODUCTION

Time-domain analysis methods for magnetic resonance spectroscopy have experienced considerable development during the past years (*1*). Different time-domain quantitation methods have been developed to avoid spectral distortions caused by the Fourier transform of a nonideal FID. Such characteristics of the FID can be incorporated in the time-domain model function, which gives rise to more-accurate parameter estimates. These methods comprise linear-prediction (LP) methods such as linear prediction combined with singular-value decomposition (LPSVD) (*2, 3*), state-space methods such as Hankel Lanczos singular-value decomposition (HLSVD) (*4*), methods using total least squares (TLS) such as Hankel TLS (HTLS) (*5*), the combination of TLS with LP (LPTLS) (*6, 7*), and others.

In addition, preprocessing methods have been proposed in order to enhance the raw data in such a way that specific requirements are met before applying a quantitation method. Here, the application of the Cadzow enhancement procedure (EP) (*8*) to MRS data leads to considerable improvements (*9*). The EP algorithm restores the Hankel structure of the data matrix which results in a reduction of the noise in the reconstructed signal. Recently, a new, improved enhancement procedure (IEP) which minimizes the filtering effects has been proposed (*10*).

All of the aforementioned SVD-based methods require the number of signal components as an input from the user. To achieve fully automatic MRS quantitation, a method that automatically and reliably determines the number of signal components is needed. In order to be successful for *in vivo* MRS data, this method must be robust even at low signal-to-noise ratios (SNRs). In this context, the application of the principle of continuous regularization (CR) (*11*) to the LPSVD analysis promises important beneficial effects. As shown in (*12*), the resulting combined LPSVD(CR) algorithm solves the problem of determining the number of components without prior knowledge successfully.

The main interest of the present paper will be directed toward the use of LPSVD(CR) in order to realize a fully automatic LPSVD analysis. It will be shown that the application of continuous regularization to LPSVD not only allows for fully automatic MRS data quantitation, but also reduces the number of algorithmic failures and results in more-accurate frequency estimates. By means of extensive Monte Carlo (MC) studies on a simulated signal, the combined LPSVD(CR) method is studied with respect to two different aspects. In the first set of MC studies, we investigate the performance of LPSVD(CR) as a stand-alone method to determine the correct number of components *and* find estimates for the spectral parameters. The automatic quantitation of LPSVD(CR) is compared to other LP-based parameter estimators that require the number of components as prior

1090-7807/97 $25.00

knowledge. Second, we consider combinations of LPSVD(CR) with other methods that first enhance the data and then perform the quantitation. In these combined methods the most important advantage of continuous regularization is exploited; i.e., it is used to estimate the number of spectral components only.

Furthermore, we also extend the application of LPSVD(CR) to the quantitation of a real-world (measured) *in vivo* ^{31}P MRS signal. Finally, the capabilities of LPSVD(CR) in terms of fully automated data-analysis protocols are summarized. All studies were performed using the magnetic resonance user interface (MRUI) software package (*13*) which is available upon request from the author (A.vdB.).

THEORY

For a detailed description of the basics of linear prediction and singular-value decomposition we refer to (*1*). Here, we only briefly mention the main steps and point out the details introduced by continuous regularization.

For the LPSVD analysis, a linear relationship between the equidistantly (Δt) sampled data points $x_n = x(n\Delta t)$ in the time domain is assumed, which may be written as (*1*)

$$x_n = \sum_{m=1}^{M} a_m x_{n\pm m} \quad \text{or} \quad \mathbf{x} = \mathbf{X}\mathbf{a}, \qquad [1]$$

where $\mathbf{x}$ and $\mathbf{X}$ represent the data vector and data matrix (dimension $L \times M$), respectively. The information about the system in question is contained in the LP coefficients a_m. A close relationship between the a_m values and the spectral parameters exists if the time-domain data can be described by the following model function (*1*),

$$x_n = \sum_{k=1}^{K} A_k \exp(i\phi_k)\exp[(\alpha_k + i\omega_k)n\Delta t], \qquad [2]$$

where K is the number of sinusoids that comprise the signal. The angular frequencies ω_k and the damping constants $\alpha_k < 0$ which occur in a nonlinear relationship can be extracted from the roots of the prediction polynomial (*1*). Finally, the estimation of the amplitudes A_k and phases ϕ_k is achieved by a least-squares fit of the model function to the signal x_n (*1*). For MRS signal analysis, this procedure was denoted LPSVD (*3*).

The solution of Eq. [1] can be written using the singular-value decomposition of the data matrix $\mathbf{X}$, according to $\mathbf{a} = \mathbf{V}\mathbf{S}^{+}\mathbf{U}^{H}\mathbf{x}$, where $\mathbf{U}$ and $\mathbf{V}$ are the orthogonal matrices of the singular vectors. $\mathbf{S}$ is the diagonal matrix of the singular values s_j [$j = 1, \ldots, \min(L, M)$], and the superscript $^{+}$ denotes the pseudo-inverse.

The dimension of the unperturbed problem, i.e., the number of components K, is reflected in the rank of the matrix $\mathbf{X}$. Since the diagonal matrix $\mathbf{S}$ has the same rank for noiseless data, only K singular values are greater than zero. However, in all realistic cases, i.e., in the presence of noise, all s_j are greater than zero. Only if K is known or can be postulated can all irrelevant noise-related singular values be set to zero. This operation is referred to as discrete regularization (DR) (*3*).

Continuous Regularization

The question arises how to get a robust least-squares (LS) solution with small norm of Eq. [1] without restricting the problem to a predetermined (known, estimated, or desired) rank. This situation suggests the introduction of the principle of continuous regularization (*11, 12*) into LPSVD. The approach of the LPSVD(CR) method consists of the introduction of a regularization parameter λ. Instead of minimizing the norm $\|\mathbf{a}\|^2$ using the truncation described above, the minimum norm condition can then be explicitly formulated, together with the demand of minimum residual deviation, in the form

$$\|\mathbf{x} - \mathbf{X}\mathbf{a}\|^2 + \lambda^2\|\mathbf{a}\|^2 \rightarrow \text{Minimum}. \qquad [3]$$

The two norms exhibit a different behavior with increasing λ, which makes its choice difficult and crucial. Hence, the regularization parameter λ has a weighting function between the desires to minimize each of the norms in Eq. [3], and this technique can be regarded as a continuous truncation of the singular values.

The regularized LS solution of Eq. [1] now leads to the formula ($L \leqslant M$ is assumed) (*11, 12*)

$$\mathbf{a}_\lambda = \mathbf{V}\mathbf{S}_\lambda^{+}\mathbf{U}^{H}\mathbf{x} = \sum_{j=1}^{M} \frac{s_j}{s_j^2 + \lambda^2}\,\mathbf{v}_j(\mathbf{u}_j^{H}\mathbf{x}). \qquad [4]$$

For a suitably chosen λ, the disturbing effect of the small singular values is avoided and a regular noise suppression is performed.

Different strategies for estimating an optimal regularization parameter λ have been proposed. For our algorithm we use the discrepancy method (*12*). This means that the greatest λ is determined for which $\|\mathbf{x} - \mathbf{X}\mathbf{a}_\lambda\|^2 = \sigma^2$ holds, where σ^2 is the variance of the noise. This approach is justified since a further increase of λ would lead to a loss of spectral information due to the oversmoothing. A further decrease of λ, on the other side, would result in the inclusion of noise features in the solution. For all LPSVD(CR) studies in the present paper, an accurate and reliable implementation of the discrepancy method by means of a simplex routine (*14*) was used. This routine provides the value of λ which mini-

mizes the difference between the residual deviation and the estimated variance of the noise.

Next, the number of spectral components K is determined from the distribution of the polynomial roots in the complex plane. Using backward LP, the K signal-related roots fall outside the unit circle, and the noise-related ones lie inside (*3*). For a reliable separation of signal and noise by this procedure, the improved precision of the LP coefficients obtained by continuous regularization is necessary because the roots of a polynomial of high order are sensitive to its coefficients. This separation can be further refined by including a number of supposed noise roots in the polynomial and using a statistical significance test on the estimated amplitudes. For the studies presented here, the latter has not been applied.

TLS Methods and Improved Enhancement Procedure

In the first set of MC studies, LPSVD(CR) is compared with the common LPSVD with discrete regularization (*3*), the combination of EP with LPSVD (*9*), and the combination of TLS with LP (LPTLS) (*6, 7*). The essential difference between LPSVD and LPTLS is that, in the latter algorithm, the SVD of the matrix $[\mathbf{X}, \mathbf{x}]$ instead of $\mathbf{X}$ is truncated to rank K and the minimum-norm total-least-squares solution is calculated. Although LPSVD, EPLPSVD, and LPTLS are regarded as black-box methods, they use the information about the number of spectral components as prior knowledge.

For the second set of MC studies, the previously suggested method of LPSVD(CR) combined with EPLPSVD (*12*) is compared with two implementations of the new combination of LPSVD(CR), IEP (*10*), and HTLS (*5*). The new combination carries out quantitation by means of the state-space-based method HTLS. This basically amounts to truncating the SVD of the matrix $[\mathbf{X}, \mathbf{x}]$ to rank K (as in LPTLS) and then using the first K columns of the matrix of the left singular vectors to compute the total-least-squares solution. It has been shown (*5*) that, in particular, the damping factor estimates at low SNR improve substantially, thereby also leading to improved accuracy of amplitude and phase estimates. The recently proposed IEP method (*10*) exploits the filtering interpretation of SVD-based iterative signal enhancement algorithms to further improve their performance.

An investigation of the effect of initial conditions in the EP procedure (*8*) on the enhanced signal leads to the conclusion that special care must be taken with regard to both the size $L \times M$ of the signal Hankel matrix in which the N samples are arranged and the number and size of singular values which are retained during each iteration. It was observed (*10*) that the effect of the initial conditions is much more important during the first iterations of the enhancement procedure. Therefore, it is advised, after fixing the number of singular values retained to the known rank K, to set the number of columns M to not greater than $K + 1$ during the first iteration. During the second iteration M can be increased to $2K$ while keeping the effect of the initial conditions minimal. Consequently, during the third and subsequent iterations, M can be further increased up to $N/2$. When M is relatively small, two or three iterations can be considered, rather than one in order to improve performance. For ease of understanding, the IEP algorithm is outlined below:

Given: N samples x_n, $n = 0, \ldots, N-1$ and $M_{\max}$ different column sizes M_j of iterations

For $j = 1, \ldots, M_{\max}$
For $k = 1, \ldots, n_j$

1. Arrange the N samples x_n, $n = 0, \ldots, N-1$ into a $M_j \times (N - M_j + 1)$ Hankel matrix $\mathbf{H}$, with $x_0, \ldots, x_{N-p}$ in its first row and $x_{N-p}, \ldots, x_{N-1}$ in its last column.
2. Compute the SVD

$$\mathbf{H} = \sum_{i=1}^{M_j} s_i u_i v_i^{\mathrm{H}}, \quad s_1 \geqslant \cdots \geqslant s_{M_j} \geqslant 0, \qquad [5]$$

and truncate to rank $K < M_j$:

$$\mathbf{H}_K = \sum_{i=1}^{K} s_i u_i v_i^{\mathrm{H}}. \qquad [6]$$

3. Replace x_n by $\hat{x}_n$, obtained by arithmetic averaging along the nth cross diagonal of the non-Hankel matrix $\mathbf{H}_K$ for all $n = 0, \ldots, N-1$.

A further improvement can in some cases be obtained by replacing the first M_{j-1} samples affected by the initial conditions by the corresponding samples of the original signal. These are only slightly contaminated by noise and can be used as accurate estimates of the corresponding noise-free samples. This alternative algorithm, denoted by IEP(Re), is outlined as the IEP algorithm, provided that the third step of the upper iteration is performed only for $n = M_j, \ldots, N-1$. The first implementation of the new combination LPSVD(CR), IEP, and HTLS uses no sample replacement, whereas the sample replacement (Re) was applied in the second combination LPSVD(CR), IEP(Re), and HTLS.

METHODS

For the investigation of the performance of LPSVD(CR) in comparison with other SVD-based methods, two sets of Monte Carlo studies were performed. These MC studies were carried out on a simulation signal that was designed in order to represent an *in vivo* MRS signal as closely as

TABLE 1

Simulation Parameters, Based on the Fit of an *in Vivo* ^{31}P MRS Signal: Frequencies ω_k, Damping Factors α_k, Amplitudes A_k, and Phases ϕ_k of the 11 Components

Component k	$\omega_k/2\pi$ [kHz]	α_k [kHz]	A_k [arbitrary units]	ϕ_k [degrees]	Comment
1	−0.086	0.050	75	135	β-ATP
2	−0.070	0.050	150	135	β-ATP
3	−0.054	0.050	75	135	β-ATP
4	0.152	0.050	150	135	α-ATP
5	0.168	0.050	150	135	α-ATP
6	0.292	0.050	150	135	γ-ATP
7	0.308	0.050	150	135	γ-ATP
8	0.360	0.025	150	135	PCr
9	0.440	0.286	1400	135	PDE
10	0.490	0.025	60	135	P_i
11	0.530	0.200	500	135	PME

Note. The last column identifies each component.

possible. The parameters (see Table 1) used to synthesize the simulated noiseless FID were taken from an accurate VARPRO analysis, including the application of biochemical prior knowledge about multiplet splittings, of an *in vivo* ^{31}P MRS FID from human brain (*15*). The corresponding spectrum displays specific problems such as the closely overlapping multiplets from adenosine triphosphate (ATP) and the narrow inorganic phosphate (P_i) peak wedged between the broad phosphomonoester (PME) and the very broad phosphodiester (PDE) peaks (see Fig. 1).

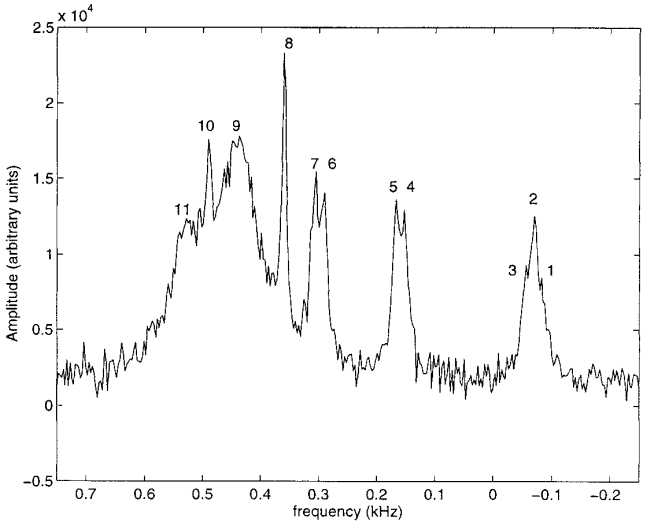

FIG. 1. Phased spectrum obtained after Fourier transform of the simulated ^{31}P signal with peak labels (noise added with standard deviation σ = 15). The original signal was acquired from a human brain.

TABLE 2

Combinations of Methods for the Second Set of Our MC Studies

Combination	Rank determination	Data enhancement	Parameter estimation
New implementation 1	LPSVD(CR)	IEP(Re)	HTLS
New implementation 2	LPSVD(CR)	IEP	HTLS
Diop *et al.* (*12*)	LPSVD(CR)	Cadzow EP (one iteration)	LPSVD(DR)

For each noise level, a set of 300 noisy signals was obtained by adding different versions of a white Gaussian noise with standard deviation σ to the noiseless simulated signal. Four different noise levels (σ = 10, 15, 20, 25) were chosen to represent *in vivo* conditions, including high noise levels where the SVD-based methods started to break down. All simulated signals in the 4 × 300 Monte Carlo set contained 256 complex data points.

The first set of MC studies was carried out in order to evaluate the accuracy of the spectral-parameter estimates of all 11 components obtained by LPSVD(CR) and other LP-based methods. This investigation comprised LPSVD(CR) as well as LPSVD with (discrete) truncation of the singular values [LPSVD(DR)] (*3*), LPSVD preceded by the Cadzow EP (*9*) with one iteration (EPLPSVD), and the linear-prediction total-least-squares (LPTLS) method (*6, 7*). These comparative studies were not performed with respect to rank estimation but in terms of parameter accuracy. Therefore, for all methods other than LPSVD(CR), the known order of the simulation (11) was given as prior knowledge. In all fits, 256 complex data points arranged in nearly square matrices of size 129 × 128 were used.

As a criterion for the determination of successful runs, we used the frequency resolution. A failure occurs if not all 11 peaks are resolved within specified intervals lying symmetrically around the exact frequencies. The half-widths of these intervals are 8.6, 7.3, 8.7, 3.2, 3.2, 3.5, 3.6, 0.7, 5.6, 2.4, and 7.8 Hz, respectively. These values are derived from the Cramer–Rao lower bounds on the frequencies at that noise standard deviation where the two intervals of two neighboring peaks in the triplet touch each other.

Second, a thorough investigation of the combination of different methods was performed. The common structure of all these combinations consists of rank determination, data enhancement, and parameter estimation (see Table 2). LPSVD(CR) + EPLPSVD, as well as the new combinations LPSVD(CR) + IEP + HTLS and LPSVD(CR) + IEP(Re) + HTLS, first use continuous regularization to determine the number of components (rank). Then EP (one iteration), IEP, or IEP(Re) is used to enhance the data, and finally

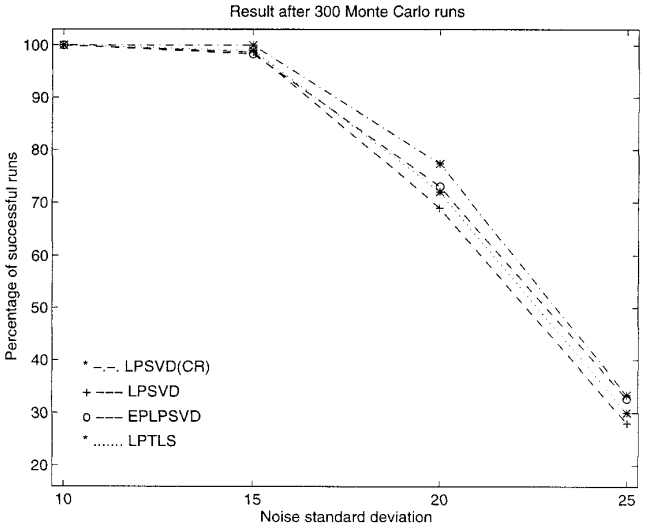

FIG. 2. MC study 1: Percentage of successful runs versus the noise standard deviation σ for LPSVD(CR), LPSVD, EPLPSVD (one iteration), and LPTLS.

parameter estimation is performed by means of common LPSVD or HTLS. The IEP procedure is carried out twice on a Hankel matrix of size 11×246 ($n_1 = 2$ and $M_1 = 11$), twice on a 20×237 matrix, twice on a 30×227 matrix, once on a 40×217 matrix, and once on an almost square 128×129 matrix. For IEP(Re), the first 11, 19, 29, 39, and 127 affected samples of the signal, respectively, were replaced by their original values. The same specifications with respect to the number of data points and matrix size as for the first set of studies were taken. Only those data combinations for which LPSVD(CR) had determined all components correctly within the specified frequency intervals were subjected to the following steps of the combination. After quantitation the frequency criterion was again applied, in the same manner as for the first set.

The MC studies were realized by means of the MRUI software package developed as part of an EU research project (*13*).

Finally, LPSVD(CR) was applied to a real-world *in vivo* ^{31}P signal from a human calf muscle, recorded at 1.5 Tesla using a surface coil.

RESULTS

The results of our MC studies are presented in terms of the percentage of successful runs and the root-mean-square error (RMSE) and the bias of the parameter estimates. These statistical quantities were estimated by computing their corresponding sample values (*16*) and are plotted against the noise standard deviation σ. In the graphs, the solid line always represents the Cramer–Rao lower bounds as a measure of the theoretically achievable accuracy. Because of the exclusion of unsuccessful runs, the calculated RMSE on certain parameters may drop below that theoretical limit.

Here a representative selection of the results is shown, focusing on those peaks of the spectrum which are most difficult to resolve. These are the components 1 to 3 (β-ATP triplet) and, because of its large damping factor, peak 9 (PDE).

Performance of the LP Parameter Estimation Methods

As follows from Fig. 2, LPSVD(CR) has the highest percentage of successful runs at all noise levels which is equivalent to the lowest failure rate. At noise level 15, there are already a few cases where not all 11 components are found correctly by LPSVD(DR), EPLPSVD, and LPTLS, whereas LPSVD(CR) produces no failure. For noise levels 20 and 25 the difference in the failure rates becomes more significant. These results were obtained even though LPSVD(CR) must perform rank determination *and* parameter estimation, whereas the order of the simulation (11) was given as prior knowledge to all other methods. It was observed that the occurrence of a failure is always because the triplet is not resolved (mostly only two components are found). In these cases LPSVD(CR) detects only 10 (or even 9) peaks, while the other methods include additional noise peaks in the fit.

In terms of parameter estimation, LPSVD(CR) exhibits a lower RMSE on the frequency and phase estimates, but not on the estimated amplitudes and dampings (Figs. 3 to 6). It can also be observed that LPSVD(CR) generally shows a larger bias (see Fig. 7), which is an inherent property of

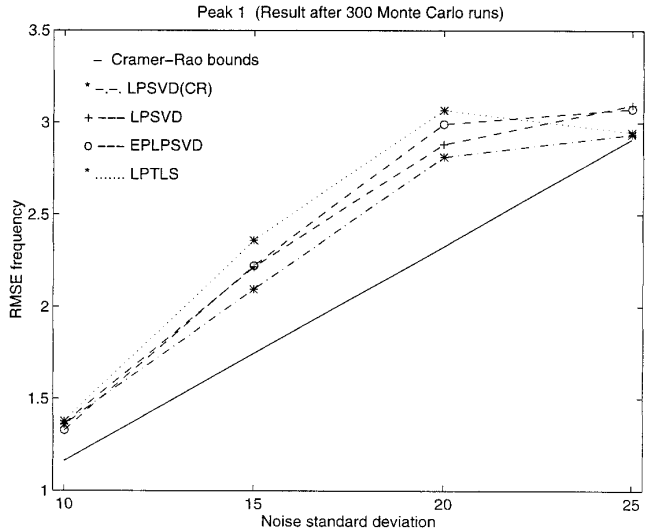

FIG. 3. MC study 1: RMSE frequency for peak 1 of the simulated ^{31}P signal for LPSVD(CR), LPSVD, EPLPSVD (one iteration), and LPTLS.

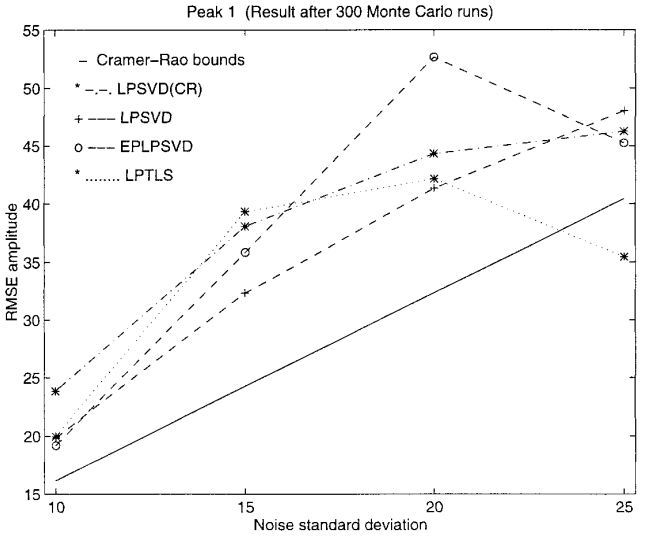

FIG. 4. MC study 1: RMSE amplitude for peak 1 of the simulated ^{31}P signal for LPSVD(CR), LPSVD, EPLPSVD (one iteration), and LPTLS.

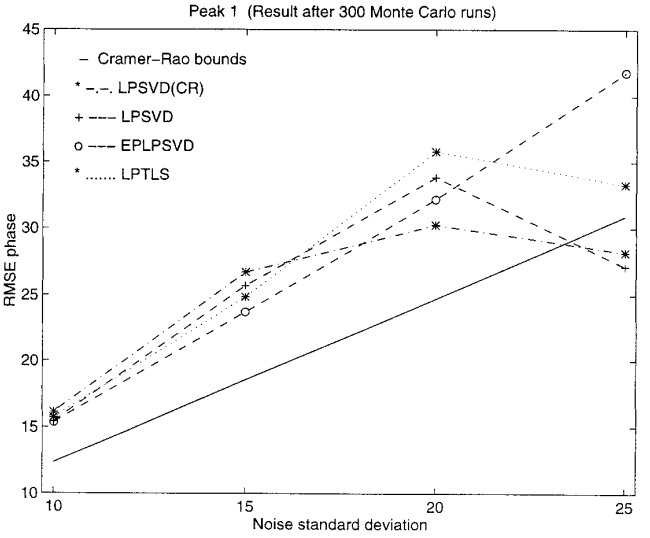

FIG. 6. MC study 1: RMSE phase for peak 1 of the simulated ^{31}P signal for LPSVD(CR), LPSVD, EPLPSVD (one iteration), and LPTLS.

regularization methods. This increase in the bias as compared to other methods is accepted because the variance of the parameter estimates is decreased simultaneously. This advantageous effect of the regularization technique leads to a desired reduction of the RMSE.

The RMSE on the parameter estimates for the β-ATP triplet as shown in Figs. 3 to 6 (for one representative component of the triplet) demonstrates that the RMSEs for frequency and phase benefit from the use of continuous regularization [i.e., the values for LPSVD(CR) are closest to the Cramer–Rao lower bounds]. These findings apply to all frequency estimates of this triplet and both ATP doublets. For a separated peak, such as the phosphocreatine (PCr) peak, the estimates obtained by all methods are very close to each other. On the other hand, for the PDE peak with its large damping, the RMSE of the frequency for EPLPSVD and LPTLS is slightly smaller than that for LPSVD(CR) (not shown here). This can probably be attributed to the fact that the estimated signal pole is dominated by the damping factor.

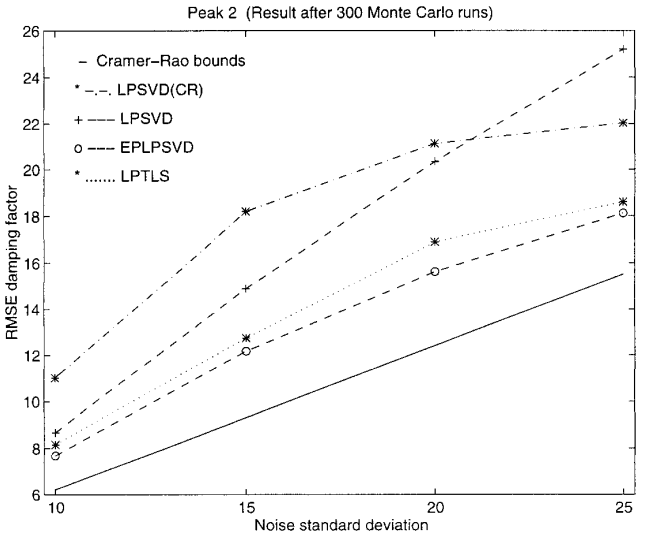

FIG. 5. MC study 1: RMSE damping factor for peak 2 of the simulated ^{31}P signal for LPSVD(CR), LPSVD, EPLPSVD (one iteration), and LPTLS.

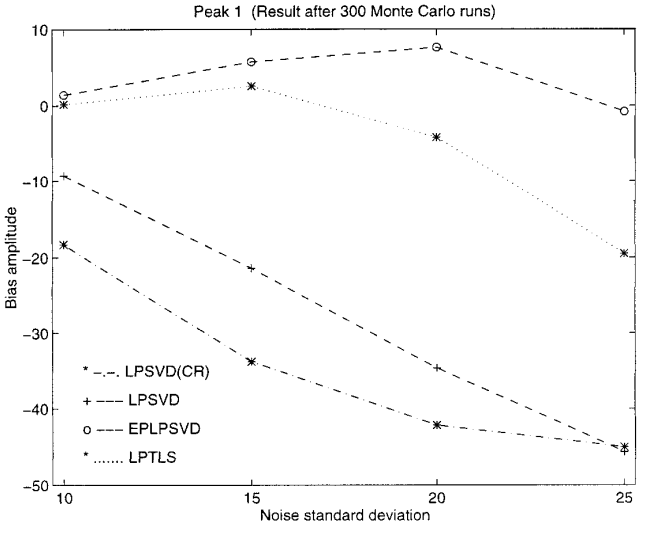

FIG. 7. MC study 1: Bias amplitude for peak 1 of the simulated ^{31}P signal for LPSVD(CR), LPSVD, EPLPSVD (one iteration), and LPTLS (true value: 75). The results for peak 3 are very similar whereas for peak 2 a positive bias was obtained for all LP-based methods.

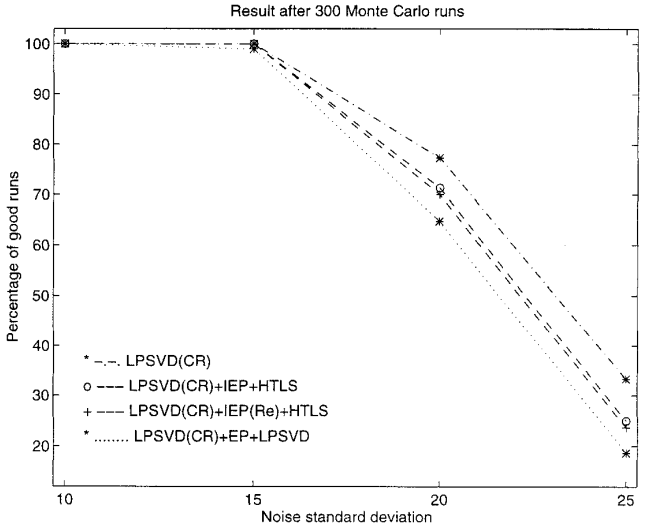

FIG. 8. MC study 2: Percentage of successful runs versus the noise standard deviation σ for the methods mentioned in Table 2.

Concerning the phases (see Fig. 6 for the phase of peak 1), the same assertions as for the frequencies hold. Again for all peaks, except the PDE and P_i peaks, LPSVD(CR) yields the lowest value for the RMSE (which for the PCr peak is close to the values obtained by all other methods again). Moreover, for the PDE and P_i peaks, the phase estimates obtained by LPSVD(CR) also show a slightly larger RMSE than the estimates obtained by EPLPSVD, LPTLS, and LPSVD.

As shown in Fig. 4, for the amplitudes (i.e., the integrated area under the peaks) we found a higher RMSE with LPSVD(CR) than with the other methods. This finding, demonstrated here for component 1, is similar for all multiplet components and for the overlapping peaks. The larger bias for the LPSVD(CR) amplitude estimates can be seen from Fig. 7. From this it is obvious that the outside component of the triplet (peak 1) is underestimated (which also applies to the other outside component 3). In contrast to this, the middle component (peak 2) is overestimated (not shown here). From our findings, this appears to be a general trend for the nonenhanced LP-based methods LPSVD, LPSVD(CR), and LPTLS.

The damping factor estimates are generally better for EPLPSVD and LPTLS than for LPSVD(CR), as shown in Fig. 5 for peak 2. Only at noise level 25 does LPSVD(CR) perform better than LPSVD. The findings concerning the damping factors are again similar for all peaks. As amplitude estimates are most important in spectral quantitation, the bias of the parameters is shown only for the amplitude of peak 1 (Fig. 7).

Summarizing, we can state that LPSVD(CR) reliably determines the correct number of spectral components, thus enabling automatic spectral quantitation. The application of LPSVD(CR) to our simulation example results in a reduced failure rate for correctly estimating all 11 frequencies. Parameter estimation for signals containing multiplets and overlapping peaks is possible as well. The parameter accuracy is different for frequencies and phases on the one hand and amplitudes and dampings on the other. That is, for the frequency and phase estimates, but not for amplitudes and dampings, we obtained the lowest RMSE with LPSVD(CR). The parameter estimates of the PDE peak showed a different behavior, which may indicate a dependence on the peak type (value of damping factor). These findings suggest a combination of LPSVD(CR) with other methods for more accurate parameter estimation in every case.

Performance of Automatic Combinations

Figure 8 shows the percentage of successful runs for the two implementations of the new combination which are LPSVD(CR) + IEP + HTLS and LPSVD(CR) + IEP(Re) + HTLS in comparison to the previously published combination consisting of LPSVD(CR) + EPLPSVD (*12*) (see Table 1) and LPSVD(CR) alone. It is evident that both of the new analysis schemes have fewer failures at every noise level than the previously suggested combination LPSVD(CR) + EPLPSVD. For comparison, the values for LPSVD(CR) alone are also displayed, showing an even lower failure rate than both the new combinations. This must be considered the trade-off for more accurate parameter estimates. The first source of failures [LPSVD(CR) not finding all 11 components in the specified frequency intervals] is identical for every combination. Therefore, the higher number of successful runs for both implementations of the new protocol than for the previously suggested one is due to the better performance of the new IEP and HTLS. The data enhancement by IEP and the parameter estimation by HTLS lead to both a higher percentage of successful runs *and* more-accurate parameter estimates. So their combination with LPSVD(CR) has two beneficial effects.

This can be seen in Figs. 9 to 11 where the RMSE of the parameter estimates for one side peak of the β-ATP triplet (component 1 or 3, respectively) is shown. Again, this can be considered representative for other multiplet peaks, too, as those results are very similar. For the amplitude estimates, the lower RMSE obtained by the new combinations of LPSVD(CR) + [IEP or IEP(Re)] + HTLS is evident in Fig. 10. This RMSE is significantly lower than those for the combination of LPSVD(CR) + EPLPSVD and for LPSVD(CR) alone (we again emphasize that the exclusion of unsuccessful runs is the reason why RMSE values at noise level 25 may drop below the Cramer–Rao lower bounds).

Figure 11 displays the RMSE of the damping factor esti-

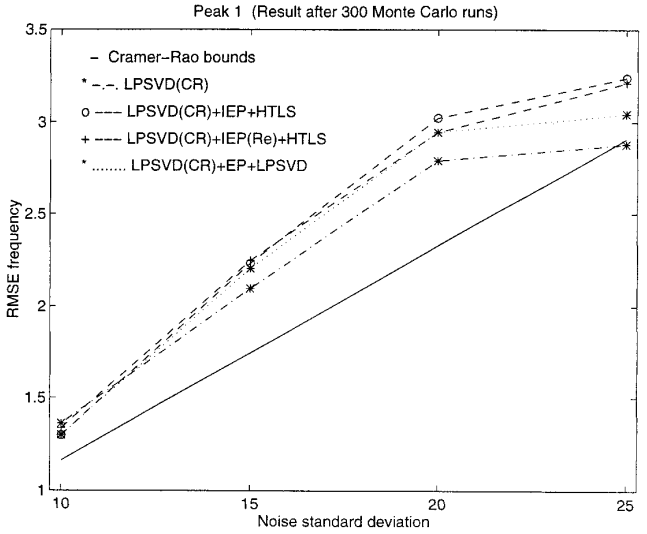

FIG. 9. MC study 2: RMSE frequency for peak 1 of the simulated ^{31}P signal for the methods mentioned in Table 2.

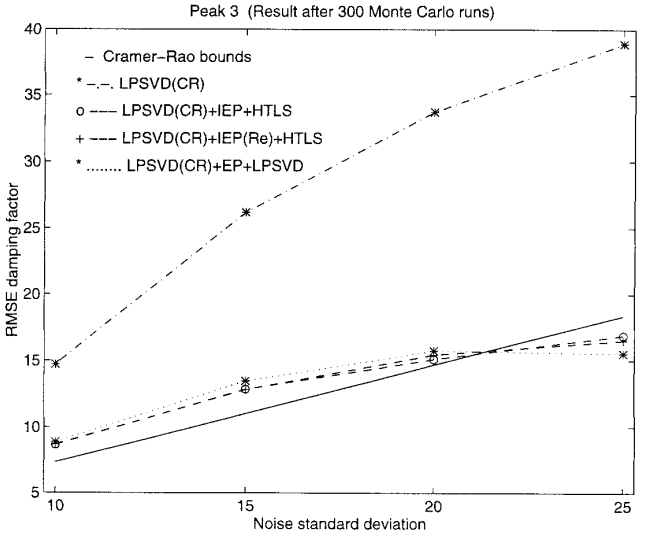

FIG. 11. MC study 2: RMSE damping factor for peak 3 of the simulated ^{31}P signal for the methods mentioned in Table 2.

mates for peak 3. Here the improvement obtained by the two new implementations, compared to LPSVD(CR) + EPLPSVD, is evident as well, although less pronounced than for the amplitudes. As with the amplitude estimates, the difference between the two new implementations is only marginal. It seems that the replacement of the data points in IEP(Re) has no big influence on the parameter accuracy for this particular signal. Taking the plot of the successful runs into account, there even seems to be a slight advantage for IEP without data replacement, but, as mentioned, the differences are only small.

Also for the frequency (Fig. 9) and phase estimates (not shown here), the RMSE is at least equal to or smaller for the new combinations than for LPSVD(CR) + EPLPSVD and LPSVD(CR) alone. Especially the frequency estimates of all methods lie close together. The new implementations generally show a smaller bias than LPSVD(CR) + EPLPSVD. The reduction in the bias is even more significant in comparison with LPSVD(CR) alone. This improvement is clearly visible for the amplitude estimates, shown here for peak 3 (Fig. 12).

The higher percentage of successful runs for the combina-

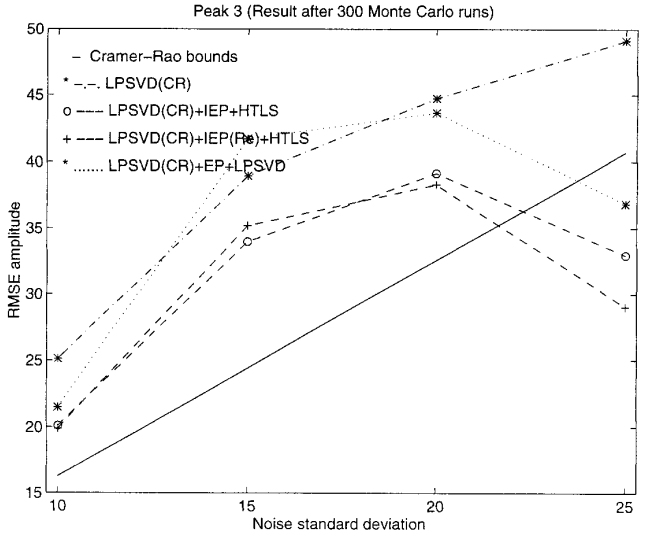

FIG. 10. MC study 2: RMSE amplitude for peak 3 of the simulated ^{31}P signal for the methods mentioned in Table 2.

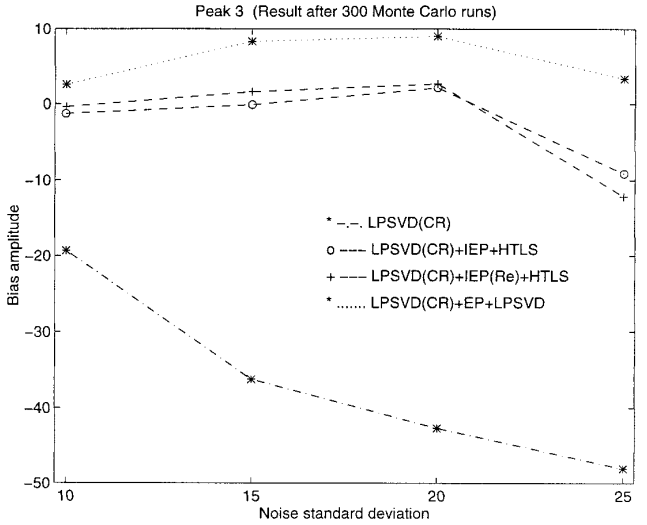

FIG. 12. MC study 2: Bias amplitude for peak 3 of the simulated ^{31}P signal for the methods mentioned in Table 2.

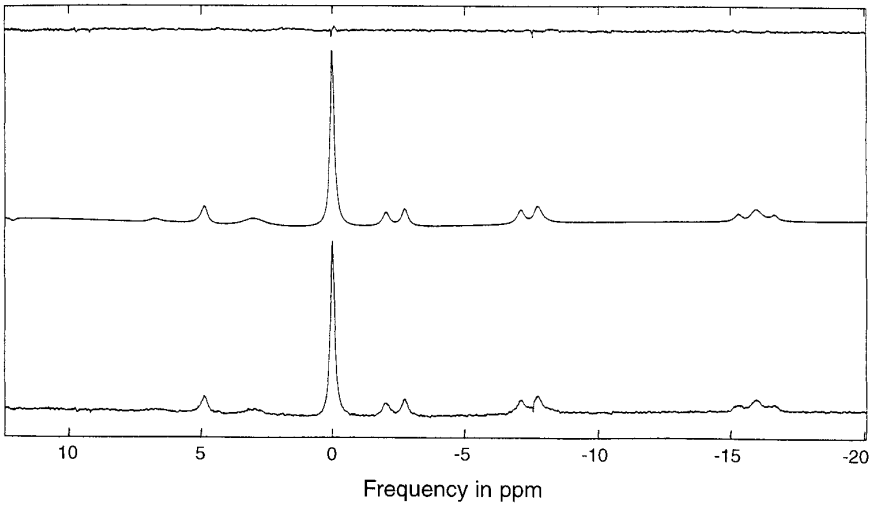

FIG. 13. Result of parameter estimation with LPSVD(CR) for real-world *in vivo* ^{31}P signal from human calf muscle. From bottom to top: FT spectra of original signal, reconstructed signal, and residual signal.

tions of LPSVD(CR) + [IEP or IEP(Re)] + HTLS implies the inclusion of more difficult runs for parameter estimation. Taking this fact into account, these new analysis schemes demonstrate a better performance than the previously suggested combination LPSVD(CR) + EPLPSVD.

Results for in Vivo ^{31}P Signal

The real-world *in vivo* ^{31}P signal from human calf muscle was chosen to illustrate the capability of LPSVD(CR) to quantify a measured signal. Figure 13 shows the results of this quantitation as performed with the MRUI software package. The FT spectra of the original signal, the reconstructed signal, and the residual between reconstructed and original signal are displayed. It is evident that all signal components were evaluated accurately using 256 data points and a nearly square matrix. The ATP triplet and doublets are well resolved, leading to a residual that contains nearly only noise. Apparently, one nonsignal component had been included by the program, near 12 ppm. However, as this fitted peak is very small (order of the noise, much smaller than any of the other fitted peaks), and lies sufficiently far outside the spectral region of interest, it will not harm the automatic analysis. It is emphasized that LPSVD(CR) *fully automatically*, without any user intervention apart from loading the signal, found the correct number of signal components, including the individual ATP multiplet components and even the low-intensity PDE (3 ppm) and PME (7 ppm) resonances.

CONCLUSIONS

In the present studies we have applied LPSVD(CR) to quantitate simulated and measured *in vivo* ^{31}P signals. These signals present substantial difficulties for parameter estimation. We conclude that LPSVD(CR) reliably determines the number of spectral components. Furthermore, estimation of the spectral parameters is possible. In particular, RMSE values for frequency and phase estimates benefit from the use of continuous regularization. For more-accurate parameter estimation a combination with other methods is suggested.

Here, by determining the number of components, LPSVD(CR) offers the possibility for fully automated data-analysis schemes. After having determined the model order with LPSVD(CR), a more-accurate parameter estimation is best carried out by HTLS preceded by a recently presented improved enhancement procedure. The new, fully automatic implementation LPSVD(CR) + [IEP or IEP(Re)] + HTLS performs significantly better than combinations of a similar structure previously used. They have a higher percentage of good runs *and* lower RMSE values for the parameter estimates. Finally, these new methods can be easily used via the MRUI software, which lowers their application threshold even more.

ACKNOWLEDGMENTS

This research was carried out as part and with the support of the EU project ''Human Capital and Mobility/Networks'' (HCM-CHRX-CT94-0432). S. Van Huffel is a Research Associate with the NFWO (Belgian National Fund for Scientific Research). The authors thank Dirk van Ormondt for his guidance of the work and Leentje Vanhamme, Sophie Cavassila, Hua Chen, and Wolfgang Kölbel for their assistance with the software and inspiring discussions. The authors are grateful to T. Binzoni, E. Hiltbrand, and P. Cerretelli from the Departments of Physiology and Radiology, University of Geneva, Switzerland, and the CIGABIN, University of Padova, Italy, for providing the *in vivo* ^{31}P MRS data set. This work was carried out at ESAT-SISTA, Katholieke Universiteit Leuven, Heverlee, Belgium.

REFERENCES

1. R. de Beer and D. van Ormondt, ''NMR Basic Principles and Progress,'' Vol. 26, M. Rudin, Berlin, 1992.
2. R. Kumaresan and D. W. Tufts, *IEEE Trans.* **ASSP-30,** 833 (1982).
3. H. Barkhuijsen, R. de Beer, W. M. M. J. Bovée, and D. van Ormondt, *J. Magn. Reson.* **61,** 465 (1985).
4. W. W. F. Pijnappel, A. van den Boogaart, R. de Beer, and D. van Ormondt, *J. Magn. Reson.* **97,** 122 (1992).
5. S. van Huffel, H. Chen, C. Decanniere, and P. van Hecke, *J. Magn. Reson.* **110,** 228 (1994).
6. C. F. Tirendi and J. F. Martin, *J. Magn. Reson.* **85,** 162 (1989).
7. S. van Huffel, L. Aerts, J. Bervoets, J. Vandewalle, C. Decanniere, and P. van Hecke, *in* ''Signal Processing VI: Theories and Applications'' (J. Vandewalle, R. Boite, M. Moonen, and A. Oosterlinck, Eds.), Vol. III, pp. 1721–1724, Elsevier Science, Amsterdam, 1992.
8. J. A. Cadzow, *IEEE Trans.* **ASSP-36,** 49 (1988).
9. A. Diop, A. Briguet, and D. Graveron-Demilly, *Magn. Reson. Med.* **27,** 318 (1992).
10. I. Dologlou, S. van Huffel, and D. van Ormondt, ESAT-SISTA Report TR 96-09, Department of Electrical Engineering, Katholieke Universiteit Leuven, Belgium, 1996 (in press in *Signal Process.*).
11. W. Kölbel and H. Schäfer, *J. Magn. Reson.* **100,** 598 (1992).
12. A. Diop, W. Kölbel, D. Michel, A. Briguet, and D. Graveron-Demilly, *J. Magn. Reson. B* **103,** 217 (1994).
13. A. van den Boogaart and M. Cabañas (1996), http://rmn3.uab.es/mruiwww/mrui_hom.html and D. Graveron-Demilly (1996), http://azur.univ-lyon1.fr/HCM/hcm.html.
14. J. A. Nelder and R. Mead, *Comput. J.* **7,** 308 (1965).
15. R. de Beer, P. Bachert-Baumann, W. M. M. J. Bovée, E. Cady, J. Chambron, R. Domisse, C. J. A. van Echteld, R. Marthur-De Vre, and S. R. Williams, *Magn. Reson. Imaging* **13,** 169 (1995).
16. M. G. Kendall and A. Stuart, ''The Advanced Theory of Statistics,'' 4th ed., Vol. 1, Griffin, London, 1979.